

Three-body problem in a two-dimensional Fermi gas

VUDTIWAT NGAMP RUETIKORN¹, MEERA M. PARISH^{1,2} and JESPER LEVINSSEN¹

¹ *T.C.M. Group, Cavendish Laboratory, JJ Thomson Avenue, Cambridge, CB3 0HE, United Kingdom*

² *London Centre for Nanotechnology, Gordon Street, London, WC1H 0AH, United Kingdom*

PACS 34.50.-s – Atomic and molecular scattering

PACS 31.15.ac – Few-body systems

PACS 05.30.Fk – Fermion systems (quantum statistical mechanics)

Abstract – We investigate the three-body properties of two identical \uparrow fermions and one distinguishable \downarrow atom interacting in a strongly confined two-dimensional geometry. We compute exactly the atom-dimer scattering properties and the three-body recombination rate as a function of collision energy and mass ratio $m_{\uparrow}/m_{\downarrow}$. We find that the recombination rate for fermions is strongly energy dependent, with significant contributions from higher partial waves at low energies. For $m_{\uparrow} \lesssim m_{\downarrow}$, the s -wave atom-dimer scattering below threshold is completely described by the scattering length. Furthermore, we examine the $\uparrow\uparrow\downarrow$ bound states (trimers) appearing at large $m_{\uparrow}/m_{\downarrow}$ and find that the energy spectrum for the deepest bound trimers resembles that of a hydrogen atom confined to two dimensions.

Introduction. – Ultracold atomic gases have proven to be an extremely versatile system, providing elegant realizations of a range of quantum many-body phenomena such as the BCS-BEC crossover and the Mott transition [1, 2]. In particular, the cold-atom system involves short-range interactions that can be tuned to have large scattering lengths, thus rendering the low-energy physics insensitive to the details of the interaction potentials and essentially “universal”. This has enabled the study of universal few-body physics, which in turn has had major consequences for the many-body system. For instance, the scattering length of diatomic molecules (dimers) was necessary for a complete description of the BCS-BEC crossover [3–5].

Few-body inelastic processes in the cold-atom system are also important since they limit the lifetime of the gas and constrain the densities that can be achieved in experiment. Furthermore, they can act as an indirect probe of the quantum system, e.g., the first experimental evidence for the Efimov effect [6] was deduced from three-body losses [7]. There is even the prospect of generating strongly correlated phases using few-body loss processes: dimer-dimer dissipation has already been shown experimentally to induce correlations [8], while it has recently been proposed that three-body dissipation can be used to engineer the Pfaffian state in two dimensions (2D) [9].

In this paper, we investigate the universal three-body problem of two identical \uparrow fermions and one \downarrow particle in

2D. Such an investigation is timely and important given the recent experiments on Fermi gases confined to a quasi-2D geometry [10–16]. Moreover, the few-body properties in 2D are qualitatively different from those in 3D: e.g., for identical bosons, the rate of recombination of three atoms into an atom and a dimer vanishes at low energies [17], in contrast to the 3D case. Indeed, we show here that the recombination rate for fermions has a similar dependence on energy to the case of identical bosons, but surprisingly we also find that higher partial wave contributions can be significant at low energies for both bosons and fermions, while the fermionic rate can even be larger than that for identical bosons in this regime. This result could potentially be important for any 2D experiment seeking to realize itinerant ferromagnetism [18]. Furthermore, bound states can impact the scattering properties; in particular, the presence of $\uparrow\uparrow\downarrow$ bound states (non-Efimov trimers) for mass ratios $m_{\uparrow}/m_{\downarrow} \gtrsim 3.33$ [19] is shown to lead to an enhanced p -wave scattering cross section in the scattering of a ^{40}K atom and a ^{40}K - ^6Li dimer. We additionally find that the deepest bound trimers have an energy spectrum that resembles that of a hydrogen atom confined to 2D, unlike the case in 3D where Efimov physics dominates.

Model. – In the following, we consider a two-component Fermi gas confined to 2D by a strong, approximately harmonic confinement, $V_{\uparrow,\downarrow}(z) = \frac{1}{2}m_{\uparrow,\downarrow}\omega_{\uparrow,\downarrow}^2 z^2$. The gas can be considered to be kinematically 2D when

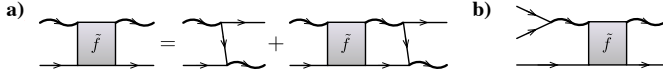


Fig. 1: (a) Illustration of the STM equation. Wavy (straight) lines are the T -matrix (atom propagator), respectively. (b) The three-body recombination process.

the temperature and Fermi energy are both smaller than the confining frequencies, $\omega_{\uparrow,\downarrow}$ (we set $k_B = \hbar = 1$). The $\uparrow\text{-}\downarrow$ interaction is characterized by a 3D s -wave scattering length a_s much larger than the van der Waals range of interatomic forces. The two species \uparrow,\downarrow are either different hyperfine states of the same atom, or single hyperfine states of different atomic species such as ${}^6\text{Li}$ and ${}^{40}\text{K}$. The low-energy scattering of two atoms is described through the s -wave scattering amplitude

$$f_{\uparrow\downarrow}(q) = \frac{2\pi}{\ln[1/(qa_{2D})] + i\pi/2}, \quad (1)$$

where \mathbf{q} is the relative momentum. We see here that the interparticle interaction is fundamentally different from the 3D case: it is energy dependent even at low energies and there always exists a bound state with binding energy $\varepsilon_B = 1/(2\mu a_{2D}^2)$, where the reduced mass $\mu^{-1} = m_{\uparrow}^{-1} + m_{\downarrow}^{-1}$. Equivalently, we can define the scattering T -matrix which describes the repeated interparticle scattering at total energy E and momentum \mathbf{q} ,

$$\mathcal{T}(\mathbf{q}, E) = \frac{2\pi/\mu}{-\ln[(E - q^2/2(m_{\uparrow} + m_{\downarrow}) + i0)/\varepsilon_B] + i\pi}.$$

Assuming that the confinement frequencies are identical for the two species, then in the limit $\varepsilon_B \ll \omega_z$, the parameter a_{2D} is related to the 3D scattering length by $a_{2D} = l_z \sqrt{\pi/B} \exp(-\sqrt{\pi/2} l_z/a_s)$, with $B \approx 0.905$ [2, 20] and confinement length $l_z = 1/\sqrt{2\mu\omega_z}$. For simplicity, in this work we restrict ourselves to the 2D limit. However, deviations from the 2D limit may be captured by the use of a two-channel model where l_z plays the role of an effective range in the two-body T -matrix [21].

Three-body problem. – We now consider the scattering of a spin- \uparrow atom with an $\uparrow\downarrow$ dimer. The process is illustrated in Fig. 1(a) and is described by the Skorniakov–Ter-Martirosian (STM) integral equation [22]. We let the incoming [outgoing] atom and dimer have four-momenta $(\mathbf{k}, \epsilon_{\mathbf{k}\uparrow})$ and $(-\mathbf{k}, E - \epsilon_{\mathbf{k}\uparrow})$ [$(\mathbf{p}, \epsilon_{\mathbf{p}\uparrow})$ and $(-\mathbf{p}, E - \epsilon_{\mathbf{p}\uparrow})$], respectively, with total energy $E = k^2/2\mu_3 - \varepsilon_B$ to ensure that the dimer is on-shell. Here we define $\epsilon_{\mathbf{k}\uparrow,\downarrow} = k^2/2m_{\uparrow,\downarrow}$ and the atom-dimer reduced mass $\mu_3^{-1} = (m_{\uparrow} + m_{\downarrow})^{-1} + m_{\uparrow}^{-1}$. With these definitions, the STM equation in 2D reads

$$\tilde{f}_{\ell}(k, p) = \zeta h(k, p) \left[g_{\ell}(k, p) - \int \frac{q dq}{2\pi} \frac{g_{\ell}(p, q) \tilde{f}_{\ell}(k, q)}{q^2 - k^2 - i0} \right]. \quad (2)$$

The atom-dimer scattering preserves angular momentum and we have used this to decouple the scattering amplitude

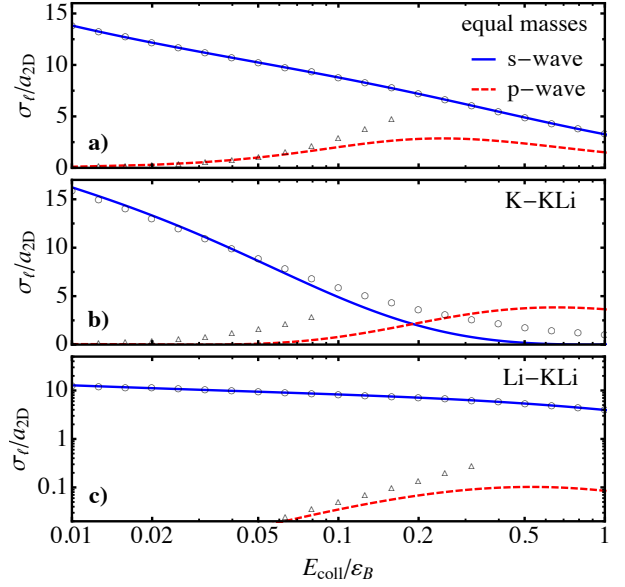


Fig. 2: (Color online) s - and p -wave elastic scattering cross sections for three different mass ratios. Circles and triangles correspond to the low-energy asymptotic behavior, Eq. (5). Note the log-scale in (c).

\tilde{f} into partial waves, denoted by $\ell = 0$ for s -wave, $\ell = 1$ for p -wave, etc. The projection of the spin- \downarrow atom propagator onto the ℓ 'th partial wave is given by

$$g_{\ell}(p, q) = \int_0^{2\pi} \frac{\cos(\ell\phi) d\phi/2\pi}{E - \epsilon_{\mathbf{p}\uparrow} - \epsilon_{\mathbf{q}\uparrow} - \epsilon_{\mathbf{p}+\mathbf{q}\downarrow} + i0}, \quad (3)$$

with ϕ the angle between \mathbf{p} and \mathbf{q} . We define the function $h(k, p) \equiv (k^2 - p^2)\mathcal{T}(\mathbf{p}, E - \epsilon_{\mathbf{p}\uparrow})$ to separate out the simple pole of the two-particle propagator occurring at $|\mathbf{k}| = |\mathbf{p}|$. We also include the factor ζ describing the quantum statistics. It takes the value -1 when the spin- \uparrow particles are fermions, $+2$ for three identical bosons, and $+1$ in the case of heteronuclear bosons with negligible $\uparrow\text{-}\uparrow$ interaction.

Elastic atom-dimer scattering. – The elastic scattering cross section in partial wave ℓ takes the form [23–25]

$$\sigma_{\ell}^{\text{el}}(E) = \frac{|f_{\ell}(k)|^2}{4k} (2 - \delta_{\ell,0}). \quad (4)$$

Note that this has dimensions of length in 2D. The partial wave scattering amplitudes are related to the solutions of Eq. (2) by $f_{\ell}(k) = \tilde{f}_{\ell}(k, k)$. Figure 2 shows the s - and p -wave scattering cross sections as a function of collision energy, $E_{\text{coll}} = k^2/2\mu_3$, for equal masses and for the mass ratios corresponding to a ${}^6\text{Li}$ - ${}^{40}\text{K}$ heteronuclear Fermi mixture. We see that s -wave scattering always dominates when $m_{\uparrow} \leq m_{\downarrow}$, while p -wave scattering becomes dominant for the K-KLi atom-dimer scattering when $E_{\text{coll}}/\varepsilon_B \geq 0.2$. This is related to a p -wave trimer state crossing the atom-dimer continuum at the mass ratio 3.33, leading to a resonant enhancement of p -wave scattering. A similar enhancement of p -wave scattering was

predicted in 3D [26] for the K-KLi system due to the appearance of a trimer at a mass ratio of 8.2 [27]. The presence of trimers in higher odd partial waves in 2D at large mass ratio [19] will likewise lead to a resonantly enhanced atom-dimer interaction.

In the low-energy limit where $ka_{2D} \ll 1$, the atom-dimer s - and p -wave amplitudes may be expanded as

$$f_s(k) \approx \frac{2\pi}{\ln[1/(ka_{ad})] + i\pi/2}, \quad f_p(k) \approx 4s_{ad}k^2, \quad (5)$$

with the atom-dimer scattering length and surface, a_{ad} and s_{ad} , describing the s - and p -wave low-energy behavior, respectively. Matching in the regime $ka_{2D} \ll 1$, we find

$$\frac{a_{ad}}{a_{2D}} = \begin{cases} 1.26 \\ 2.29 \\ 1.02 \end{cases}, \quad \frac{s_{ad}}{a_{2D}^2} = \begin{cases} -2.92 & m_{\uparrow}/m_{\downarrow} = 1 \\ -1.54 & m_{\uparrow}/m_{\downarrow} = m_K/m_{Li} \\ -0.44 & m_{\uparrow}/m_{\downarrow} = m_{Li}/m_K \end{cases}$$

The low-energy quantities are shown as a function of mass ratio in Fig. 3. We see that the scattering length increases monotonically with $m_{\uparrow}/m_{\downarrow}$, whereas the scattering surface displays a series of divergences, related to the appearance of trimers. The atom-dimer scattering length for equal masses has also been estimated from a QMC calculation of the pairing gap in the BEC regime, but they instead obtain $a_{ad} \approx 1.7a_{2D}$ [28]. This disagreement with our exact few-body calculation is most likely because the equation of state has a complicated dependence on a_{ad} , making the determination of a_{ad} difficult. For large $m_{\uparrow}/m_{\downarrow}$, we find $a_{ad} \approx 0.845a_{2D} \ln(\sqrt{2}e^{\gamma/2}m_{\uparrow}/\mu)$, with the Euler constant $\gamma \approx 0.577$. A logarithmic dependence on mass ratio was also found in the 3D case [29]. Additionally, from Eq. (5) we calculate the asymptotic behavior of the cross section and this is shown in Fig. 2. A surprising feature is that the s -wave scattering cross section is completely determined by a_{ad} for $m_{\uparrow} \lesssim m_{\downarrow}$, even though all coefficients in the low-energy expansion of the scattering amplitude would be expected to have a characteristic scale of a_{2D} . A similar result appears in 3D for $m_{\uparrow} = m_{\downarrow}$ [30].

Trimers. – We now turn to trimers, which formally appear as an energy pole in Eq. (2) for odd partial waves. The spectrum of p -wave trimers as a function of mass ratio is shown in Fig. 4. The appearance of trimers at large mass ratios in 2D may be elucidated by applying the Born-Oppenheimer approximation [31], which shows that the effective potential between heavy fermionic atoms mediated by the light atom at distances $\lesssim a_{2D}$ is similar to the electron potential in a hydrogen atom confined to 2D. To see this, assume that the state of the light atom at position \mathbf{r} adiabatically adjusts itself to the positions $\pm\mathbf{R}/2$ of the heavy atoms. Atom-dimer scattering in odd partial wave channels is described by the symmetric light-atom wavefunction [29]

$$\psi_{\mathbf{R}}(\mathbf{r}) \propto K_0(\kappa(R)|\mathbf{r} - \mathbf{R}/2|) + K_0(\kappa(R)|\mathbf{r} + \mathbf{R}/2|), \quad (6)$$

where the modified Bessel function of the second kind $K_0(\kappa r)$ is the decaying solution of the free Schrödinger

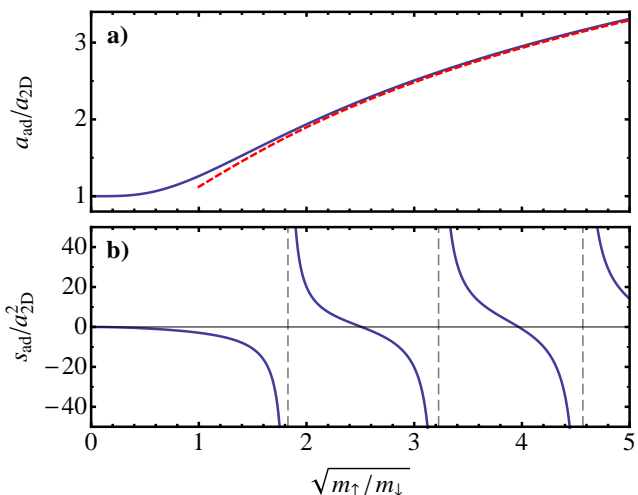


Fig. 3: (Color online) (a) Scattering length and (b) surface as a function of mass ratio. The dashed line in (a) is calculated from the asymptotic expression in the limit of a large mass imbalance. The vertical dashed lines in (b) signify the appearance of trimers.

equation with energy $\epsilon(R) = -\kappa(R)^2/2m_{\downarrow}$. The singularities at the positions of the heavy atoms satisfy the Bethe-Peierls boundary condition in 2D: For $\tilde{\mathbf{r}} = \mathbf{r} \pm \mathbf{R}/2$ this is $[\tilde{\mathbf{r}}(\psi)_{\tilde{\mathbf{r}}}/\psi]_{\tilde{\mathbf{r}} \rightarrow \mathbf{0}} = 1/\ln(\tilde{r}e^{\gamma}/2a_{2D})$. Using the asymptotic form, $K_0(x) \stackrel{x \rightarrow 0}{\approx} -\ln(xe^{\gamma}/2)$, we then obtain the condition $\ln\left(-\frac{\epsilon(R)}{\epsilon_B}\right) = 2K_0\left(\sqrt{-\frac{\epsilon(R)}{\epsilon_B}}\frac{R}{a_{2D}}\right)$.

In the second stage of the Born-Oppenheimer approximation, the Schrödinger equation of the heavy particles is solved using $\epsilon(R)$ as the effective interaction potential. In the limit $R \ll a_{2D}$, the potential becomes $\epsilon(R) \approx -\frac{2\epsilon_B}{e^{\gamma}}\frac{a_{2D}}{R}$. Thus, the spectrum of the deepest bound trimer states is hydrogen-like and given by the well-known result (appropriately shifted by the dimer binding energy) [32]

$$E_n = -\frac{m_{\uparrow}}{e^{2\gamma}m_{\downarrow}}\frac{\epsilon_B}{2(n+1/2)^2} - \epsilon_B, \quad (7)$$

with integer quantum number $n \geq \ell$. This also implies that deeply bound trimers with different ℓ are degenerate, as was found in Ref. [19]. Furthermore, we note that the wavefunction (6), and thus the above arguments, apply equally well to heteronuclear bosons in even partial waves.

A similar scenario for large mass ratios was recently predicted [33] in the context of a 3D Fermi gas close to a narrow interspecies Feshbach resonance, characterized by a large effective range R^* . The effective interaction between the two heavy fermions mediated by the light atom goes like $-1/R^2$ in the range $R^* \ll R \ll a_s$, while at shorter ranges, $R \ll R^*$, this behavior is replaced by an attractive $1/R$ potential [34], leading to a crossover from an Efimovian spectrum for the weakly bound trimers to a hydrogen-like spectrum for the deepest trimers [33].

Referring to Fig. 4, for the deepest bound states, we

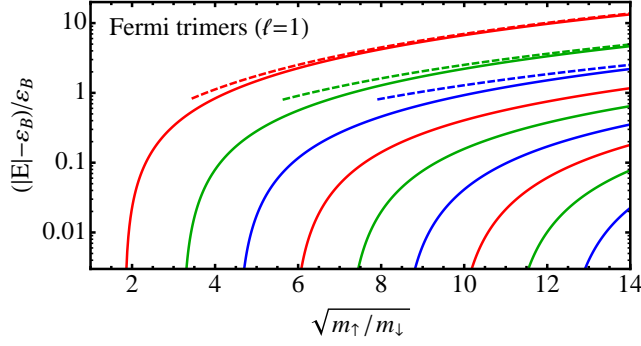


Fig. 4: (Color online) Trimer energies (solid lines) as a function of mass ratio. Our results match those of Ref. [19]. Dashed lines are the hydrogen-like spectrum, Eq. (7).

find very good agreement with the hydrogen-like spectrum (7). At a given mass ratio, the potential only supports a finite number of bound states proportional to the number of nodes of the heavy-atom wavefunction that fit in the hydrogen-like part of the potential, $R \lesssim a_{2D}$. We estimate this number by noting that in this regime the wavefunction of heavy atoms is proportional to the Bessel function $J_{2\ell}(2\sqrt{e^{-\gamma}(m_\uparrow/m_\downarrow)}R/a_{2D})$. Since the wavefunction acquires an additional node each time the argument increases by π , the number of trimers is proportional to $\sqrt{m_\uparrow/m_\downarrow}$. This feature is clearly observed in Fig. 4.

Three-body recombination. – Turning now to inelastic scattering, three-body recombination is the process whereby two atoms bind into a shallow dimer with the released energy carried away by a third atom. To extract the recombination rate from the atom-dimer scattering amplitude, we consider the recombination process in reverse. This is illustrated in Fig. 1(b) which shows how the recombination process is described by the same diagram as inelastic atom-dimer scattering – a process in which no dimer remains after the scattering. The total recombination rate is therefore proportional to the atom-dimer inelastic scattering cross section [35] $K(E) = v_{\text{ad}} \frac{\Phi_{\text{ad}}}{\Phi_{\text{aaa}}} \sum_\ell \sigma_\ell^{\text{inel}}(E)$, where the atom-dimer relative speed is $v_{\text{ad}} = k/\mu_3$ and the sum is over all partial waves. The phase space of an atom-dimer pair Φ_{ad} and three atoms Φ_{aaa} are given in the appendix. The inelastic scattering cross section $\sigma_\ell^{\text{inel}}$ is obtained by subtracting the elastic from the total cross section, which is related to the imaginary part of the scattering amplitude through the optical theorem [23, 24]

$$\sigma_\ell^{\text{tot}}(E) = -\frac{1}{k} \Im[f_\ell(k)](2 - \delta_{\ell,0}). \quad (8)$$

Thus we arrive at the recombination rate

$$K(E) = \pi\rho! \frac{2m_\uparrow + m_\downarrow}{m_\uparrow^2 m_\downarrow} \frac{2k}{E} \sum_\ell \sigma_\ell^{\text{inel}}(E), \quad (9)$$

with the degeneracy factor $\rho = 2$ if $\uparrow \neq \downarrow$, *i.e.* for fermions or heteronuclear bosons, and $\rho = 3$ for identical bosons.

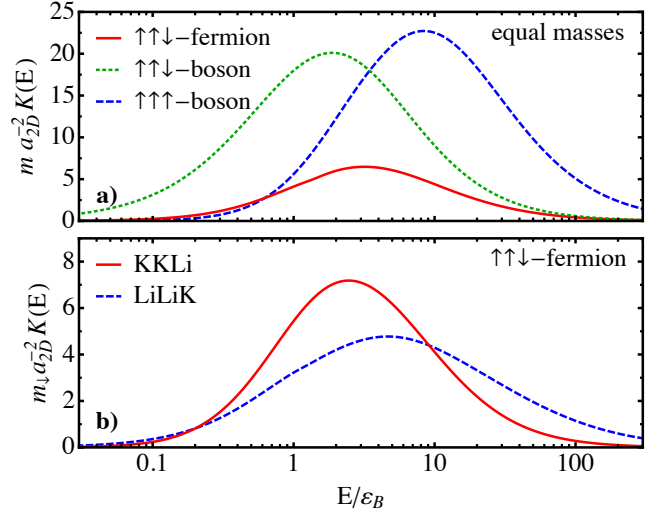


Fig. 5: (Color online) The recombination rate as a function of energy for (a) $m_\uparrow = m_\downarrow$ and (b) the Li-K heteronuclear mixture. In the low energy limit $E/\varepsilon_B \ll 1$, the result for identical bosons matches the purely s -wave calculation in Ref. [17].

Figure 5 shows the energy-dependent recombination rate for atoms of equal masses and for the Li-K fermionic mixture. The rate is expected to be maximal for scattering at energies of the order of the energy of the bound pair in the final state, ε_B , and indeed this is seen to be the case. Moreover, we find that several partial waves are of the same order of magnitude in this regime. Surprisingly, we find that the d -wave channel dominates recombination of K-K-Li fermionic atoms and of three identical bosons for most of the plotted energy range, whereas the p -wave channel is dominant for equal mass and Li-Li-K fermions, as well as for heteronuclear bosons. Similar results were found for three identical bosons in 3D [35].

On the other hand, in the low energy limit of $E \ll \varepsilon_B$ we find that the fermionic rate is comparable to that of identical bosons. This is manifestly different from the behavior in 3D, where the low-energy recombination rate approaches a constant in the three-boson problem [36] while it is suppressed in Fermi systems due to Pauli blocking with $K(E \rightarrow 0) \sim E$ [29]. The low-energy behavior of the 2D recombination rate originates from the logarithmic form of the scattering amplitude, see Eq. (1). In all cases we find that $K(E)$ approaches zero faster than E , which is a purely two-dimensional feature.

To obtain an experimentally accessible quantity, we average $K(E)$ over energy with an appropriate thermal distribution. This yields the event rate constant per unit volume α , defined such that the number of recombination events per unit volume per unit time is $\alpha n_\uparrow^2 n_\downarrow$ for the process $\uparrow + \uparrow + \downarrow \rightarrow \uparrow + \uparrow\downarrow$ in a two-component Fermi mixture. When the kinetic energy of the resulting particles is greater than the height of the trap, the loss rate is given by $\dot{n}_\uparrow = -2\alpha_{\uparrow\uparrow\downarrow} n_\uparrow^2 n_\downarrow - \alpha_{\downarrow\uparrow\uparrow} n_\downarrow^2 n_\uparrow$. At sufficiently high temperatures, we employ the Boltzmann distribution

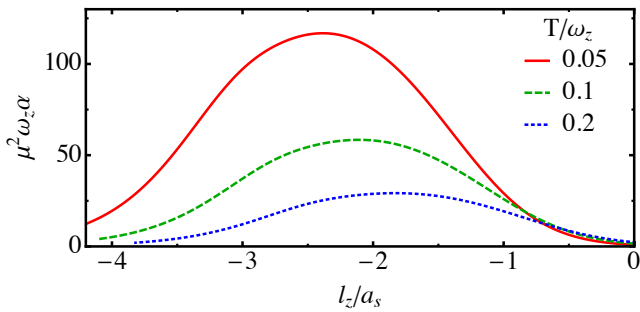


Fig. 6: (Color online) The event rate constant α for fermions with $m_\uparrow = m_\downarrow$ as a function of (inverse) 3D scattering length.

which gives [17, 37]

$$\alpha(T) = \frac{\int_0^\infty dE E e^{-E/k_B T} K(E)}{\rho! \int_0^\infty dE E e^{-E/k_B T}}. \quad (10)$$

This quantity is illustrated in Fig. 6 for a range of typical temperatures. Similar to the recombination rate, the event rate constant is expected to peak at a temperature of the order of the binding energy. Consequently, for increasing temperatures the peak value decreases as $\alpha_{\text{peak}} \sim T^{-1}$ and the peak position, $[l_z/a_s]_{\text{peak}} \sim -\ln(T)$, shifts from the BCS side of the 3D resonance towards unitarity. Note that as the binding energy decreases with decreasing l_z/a_s , the low-energy (high-energy) recombination occurs to the right (left) of the peak in Fig. 6. Towards the 3D resonance we expect corrections to our results due to deviations from the 2D limit, however these are small for the experimentally relevant parameters considered in Fig. 6 [38].

Conclusion. – At present, heteronuclear fermionic Li-K mixtures [39, 40] are promising candidates for the observation of resonantly enhanced atom-dimer scattering and trimer formation. Avenues towards observing the hydrogen-like spectrum predicted at large mass ratio include using the recently predicted Feshbach resonance in fermionic Li-Yb mixtures [41] as well as the application of a species selective optical lattice to enhance the effective mass ratio [42].

We also expect our results to be important for ongoing experiments on quasi-2D Fermi gases. In particular, three-body recombination will limit the stability of repulsive Fermi gases and potentially generate three-body correlations, thus impacting any experiment seeking to realize itinerant ferromagnetism. Moreover, it would be interesting to investigate how three-body losses might evolve into two-body losses in the presence of a Fermi sea [43, 44].

We thank D. S. Petrov, S. K. Baur, M. Köhl, and P. Massignan for fruitful discussions. JL acknowledges support from the Carlsberg Foundation and from a Marie

Curie Intra European grant within the 7th European Community Framework Programme. MMP acknowledges support from the EPSRC under Grant No. EP/H00369X/2

Appendix. – The N -particle phase space integral is defined such that

$$\Phi = \eta \int \left(\prod_{i=1}^N \frac{d^2 \mathbf{p}_i}{(2\pi)^2} \right) (2\pi)^2 \delta^{(2)} \left(\sum_{i=1}^N \mathbf{p}_i \right) \delta \left(E - \sum_{i=1}^N \frac{\mathbf{p}_i^2}{2m_i} \right), \quad (11)$$

where indistinguishability of particles gives rise to the factor $\eta \leq 1$. Using this definition, the atom-dimer and three-atom phase space is given by

$$\Phi_{\text{ad}} = \mu_3/2\pi, \quad \Phi_{\text{aaa}} = \eta \frac{E}{4\pi^2} \frac{m_1 m_2 m_3}{m_1 + m_2 + m_3}. \quad (12)$$

For three particles, $\eta = 1/\rho!$ where ρ is the number of identical particles. The phase space factors were derived in the bosonic case for equal masses in Ref. [17].

REFERENCES

- [1] GIORGINI S., PITAEVSKII L. P. and STRINGARI S., *Rev. Mod. Phys.*, **80** (2008) 1215.
- [2] BLOCH I., DALIBARD J. and ZWERGER W., *Rev. Mod. Phys.*, **80** (2008) 885.
- [3] PETROV D. S., SALOMON C. and SHLYAPNIKOV G. V., *Phys. Rev. Lett.*, **93** (2004) 090404.
- [4] BRODSKY I. V., KAGAN M. Y., KLAPTSOV A. V., COMBESCOT R. and LEYRONAS X., *Phys. Rev. A*, **73** (2006) 032724.
- [5] LEVINSSEN J. and GURARIE V., *Phys. Rev. A*, **73** (2006) 053607.
- [6] EFIMOV V., *Nuclear Physics A*, **210** (1973) 157.
- [7] KRAEMER T., MARK M., WALDBURGER P., DANZL J. G., CHIN C., ENGESER B., LANGE A. D., PILCH K., JAAKKOLA A., NÄGERL H.-C. and GRIMM R., *Nature*, **440** (2006) 315.
- [8] SYASSEN N., BAUER D. M., LETTNER M., VOLZ T., DIETZE D., GARCÍA-RIPOLL J. J., CIRAC J. I., REMPE G. and DÜRR S., *Science*, **320** (2008) 1329.
- [9] RONCAGLIA M., RIZZI M. and CIRAC J. I., *Phys. Rev. Lett.*, **104** (2010) 096803.
- [10] MARTIYANOV K., MAKHALOV V. and TURLAPOV A., *Phys. Rev. Lett.*, **105** (2010) 030404.
- [11] FRÖHLICH B., FELD M., VOGT E., KOSCHORRECK M., ZWERGER W. and KÖHL M., *Phys. Rev. Lett.*, **106** (2011) 105301.
- [12] DYKE P., KUHNLE E. D., WHITLOCK S., HU H., MARK M., HOINKA S., LINGHAM M., HANNAFORD P. and VALE C. J., *Phys. Rev. Lett.*, **106** (2011) 105304.
- [13] FELD M., FRÖHLICH B., VOGT E., KOSCHORRECK M. and KÖHL M., *Nature*, **480** (2011) 75.
- [14] SOMMER A. T., CHEUK L. W., KU M. J. H., BAKR W. S. and ZWIERLEIN M. W., *Phys. Rev. Lett.*, **108** (2012) 045302.
- [15] KOSCHORRECK M., PERTOT D., VOGT E., FRÖHLICH B., FELD M. and KÖHL M., *Nature*, **485** (2012) 619.

- [16] ZHANG Y., ONG W., ARAKELYAN I. and THOMAS J. E., *Phys. Rev. Lett.*, **108** (2012) 235302.
- [17] HELFRICH K. and HAMMER H.-W., *Phys. Rev. A*, **83** (2011) 052703.
- [18] ZHANG S. and HO T.-L., *New Journal of Physics*, **13** (2011) 055003.
- [19] PRICOUPENKO L. and PEDRI P., *Phys. Rev. A*, **82** (2010) 033625.
- [20] PETROV D. S. and SHLYAPNIKOV G. V., *Phys. Rev. A*, **64** (2001) 012706.
- [21] LEVINSEN J. and PARISH M. M., *Phys. Rev. Lett.*, **110** (2013) 055304.
- [22] SKORNIKOV G. V. and TER-MARTIROSIAN K. A., *Sov. Phys. JETP*, **4** (1957) 648.
- [23] LANDAU L. D. and LIFSHITZ E. M., *Quantum Mechanics* 3rd Edition (Butterworth-Heinemann, Oxford) 1981.
- [24] ADHIKARI S. K., *American Journal of Physics*, **54** (1986) 362.
- [25] The degeneracy comes from the quantization of angular momentum along the z -axis. In 2D, the degeneracy is 1 if $\ell = 0$ and 2 otherwise, in contrast to $2\ell + 1$ in 3D.
- [26] LEVINSEN J., TIECKE T. G., WALRAVEN J. T. M. and PETROV D. S., *Phys. Rev. Lett.*, **103** (2009) 153202.
- [27] KARTAVTSEV O. I. and MALYKH A. V., *Journal of Physics B Atomic Molecular Physics*, **40** (2007) 1429.
- [28] BERTAINA G. and GIORGINI S., *Phys. Rev. Lett.*, **106** (2011) 110403.
- [29] PETROV D. S., *Phys. Rev. A*, **67** (2003) 010703(R).
- [30] LEVINSEN J. and PETROV D., *The European Physical Journal D*, **65** (2011) 67.
- [31] BORN M. and OPPENHEIMER R., *Annalen der Physik*, **389** (1927) 457.
- [32] FLÜGGE S. and MARSCHALL H., *Rechenmethoden der Quantentheorie* (Springer-Verlag, Berlin) 1952.
- [33] CASTIN Y. and TIGNONE E., *Phys. Rev. A*, **84** (2011) 062704.
- [34] PETROV D. S., in *Many-body physics with ultra-cold gases: Lecture Notes of the Les Houches Summer Schools, vol. 94*, edited by C. SALOMON, G. V. SHLYAPNIKOV L. C., (Oxford University Press, Oxford, England) 2012.
- [35] BRAATEN E., HAMMER H.-W., KANG D. and PLATTER L., *Phys. Rev. A*, **78** (2008) 043605.
- [36] PETROV D. S., *Phys. Rev. Lett.*, **93** (2004) 143201.
- [37] MASSIGNAN P. and STOOF H. T. C., *Phys. Rev. A*, **78** (2008) 030701.
- [38] In the calculation leading to Fig. 6, we employ the two-channel model developed in Ref. [21] to model the scattering in a transverse confinement. We have checked that our results agree with the pure 2D calculation, with corrections negligible for small negative a_s/l_z and corrections of no more than 10% at the 3D resonance.
- [39] WILLE E., SPIEGELHALDER F. M., KERNER G., NAIK D., TRENKWALDER A., HENDL G., SCHRECK F., GRIMM R., TIECKE T. G., WALRAVEN J. T. M., KOKKELMANS S. J. J. M. F., TIESINGA E. and JULIENNE P. S., *Phys. Rev. Lett.*, **100** (2008) 053201.
- [40] RIDINGER A., CHAUDHURI S., SALEZ T., FERNANDES D. R., BOULOUPA N., DULIEU O., SALOMON C. and CHEVY F., *Europhys. Lett.*, **96** (2011) 33001.
- [41] BRUE D. A. and HUTSON J. M., *Phys. Rev. Lett.*, **108** (2012) 043201.
- [42] PETROV D. S., ASTRAKHARCHIK G. E., PAPOULAR D. J., SALOMON C. and SHLYAPNIKOV G. V., *Phys. Rev. Lett.*, **99** (2007) 130407.
- [43] PIETILÄ V., PEKKER D., NISHIDA Y. and DEMLER E., *Phys. Rev. A*, **85** (2012) 023621.
- [44] NGAMP RUETIKORN V., LEVINSEN J. and PARISH M. M., *Europhys. Lett.*, **98** (2012) 30005.